



ORIGINAL ARTICLE

# Neurophysiological underpinnings of an intensive protocol for upper limb motor recovery in subacute and chronic stroke patients

Michael LASSI<sup>1,2</sup>, Stefania DALISE<sup>3</sup>, Andrea BANDINI<sup>1,2,4</sup>, Vincenzo SPINA<sup>3</sup>, Valentina AZZOLLINI<sup>3</sup>, Matteo VISSANI<sup>1,2,5,6</sup>, Silvestro MICERA<sup>1,2,7</sup>, Alberto MAZZONI<sup>1,2</sup>, Carmelo CHISARI<sup>3\*</sup>

<sup>1</sup>The Biorobotics Institute, Scuola Superiore Sant'Anna, Pisa, Italy; <sup>2</sup>Department of Excellence in Robotics and AI, Scuola Superiore Sant'Anna, Pisa, Italy; <sup>3</sup>Neurorehabilitation Unit, Pisa University Hospital, Pisa, Italy; <sup>4</sup>Health Science Interdisciplinary Research Center, Scuola Superiore Sant'Anna, Pisa, Italy; <sup>5</sup>Harvard Medical School, Boston, MA, USA; <sup>6</sup>Department of Neurosurgery, Massachusetts General Hospital, Boston, MA, USA; <sup>7</sup>Bertarelli Foundation Chair in Translational Neural Engineering, Center for Neuroprosthetics and Institute of Bioengineering, École Polytechnique Fédérale de Lausanne, Lausanne, Switzerland

\*Corresponding author: Carmelo Chisari, Neurorehabilitation Unit, Pisa University Hospital, Via Paradisa, 2, 56124 Pisa, Italy.  
E-mail: [c.chisari@ao-pisa.toscana.it](mailto:c.chisari@ao-pisa.toscana.it)

*This is an open access article distributed under the terms of the Creative Commons CC BY-NC-ND license which allows users to copy and distribute the manuscript, as long as this is not done for commercial purposes and further does not permit distribution of the manuscript if it is changed or edited in any way, and as long as the user gives appropriate credits to the original author(s) and the source (with a link to the formal publication through the relevant DOI) and provides a link to the license. Full details on the CC BY-NC-ND 4.0 are available at <https://creativecommons.org/licenses/by-nc-nd/4.0/>.*

## ABSTRACT

**BACKGROUND:** Upper limb (UL) motor impairment following stroke is a leading cause of functional limitations in activities of daily living. Robot-assisted therapy supports rehabilitation, but how its efficacy and the underlying neural mechanisms depend on the time after stroke is yet to be assessed.

**AIM:** We investigated the response to an intensive protocol of robot-assisted rehabilitation in sub-acute and chronic stroke patients, by analyzing the underlying changes in clinical scores, electroencephalography (EEG) and end-effector kinematics. We aimed at identifying neural correlates of the participants' upper limb motor function recovery, following an intensive 2-week rehabilitation protocol.

**DESIGN:** Prospective cohort study.

**SETTING:** Inpatients and outpatients from the Neurorehabilitation Unit of Pisa University Hospital, Italy.

**POPULATION:** Sub-acute and chronic stroke survivors.

**METHODS:** Thirty-one stroke survivors (14 sub-acute, 17 chronic) with mild-to-moderate UL paresis were enrolled. All participants underwent ten rehabilitative sessions of task-oriented exercises with a planar end-effector robotic device. All patients were evaluated with the Fugl-Meyer Assessment Scale and the Wolf Motor Function Test, at recruitment (T0), end-of-treatment (T1), and one-month follow-up (T2). Along with clinical scales, kinematic parameters and quantitative EEG were collected for each patient. Kinematics metrics were related to velocity, acceleration and smoothness of the movement. Relative power in four frequency bands was extracted from the EEG signals. The evolution over time of kinematic and EEG features was analyzed, in correlation with motor recovery.

**RESULTS:** Both groups displayed significant gains in motility after treatment. Sub-acute patients displayed more pronounced clinical improvements, significant changes in kinematic parameters, and a larger increase in Beta-band in the motor area of the affected hemisphere. In both groups these improvements were associated to a decrease in the Delta-band of both hemispheres. Improvements were retained at T2.

**CONCLUSIONS:** The intensive two-week rehabilitation protocol was effective in both chronic and sub-acute patients, and improvements in the two groups shared similar dynamics. However, stronger cortical and behavioral changes were observed in sub-acute patients suggesting different reorganizational patterns.

**CLINICAL REHABILITATION IMPACT:** This study paves the way to personalized approaches to UL motor rehabilitation after stroke, as highlighted by different neurophysiological modifications following recovery in subacute and chronic stroke patients.

*(Cite this article as: Lassi M, Dalise S, Bandini A, Spina V, Azzollini V, Vissani M, et al. Neurophysiological underpinnings of an intensive protocol for upper limb motor recovery in subacute and chronic stroke patients. Eur J Phys Rehabil Med 2023 Nov 21. DOI: 10.23736/S1973-9087.23.07922-4)*

**KEY WORDS:** Stroke; Biomarkers; Neurophysiology; Neurological rehabilitation; Robotics.

Stroke is the third cause of disability in adults worldwide.<sup>1</sup> Although stroke survivors frequently achieve the recovery of a functional gait, the function of upper limbs often remains impaired, with a negative impact on quality of life.<sup>2, 3</sup> Defining treatments for optimal upper limb (UL) recovery is hence a key challenge for health systems.<sup>4</sup> Numerous motor control recovery strategies were proposed, including technological, pharmacological, and neuromodulatory approaches.<sup>5</sup> Specifically, rehabilitation protocols using robot-assisted therapy achieved promising results.<sup>6, 7</sup> Most of these protocols are based on motor learning principles and task-oriented exercises,<sup>8</sup> and are characterized by targeted movements and variability of tasks performed in an intensive and highly repeatable modality.<sup>9</sup> However, to date, it remains imperative to identify biomarkers of stroke recovery pertaining multiple domains (*i.e.*, clinical/functional, biomechanical, and neurophysiological) to provide a comprehensive description of the response to a specific treatment,<sup>10</sup> and design interventions based on an individual's needs. Indeed, while several studies investigated neural and biomechanical biomarkers of the recovery,<sup>11</sup> rarely the attention have been focused on the changes of brain responses at different post-stroke phases. Additionally, how the dosage and duration of rehabilitation is entangled with the time from stroke event is still a matter of debate.<sup>12</sup>

Moreover, there is no general consensus in the current literature regarding specific prescriptions of different robotic strategies, the exact characteristics of patients who could benefit from these treatments and the correct timing to use them.<sup>13</sup> Specifically, it is still greatly debated whether upper limb robot-assisted therapy could be more effective in the sub-acute or in the chronic stage of stroke, with implications on patient benefits and cost management.<sup>14</sup>

To reach these goals, it is hence necessary to reveal the entanglement between upper limb function and brain reorganization throughout the different stages of stroke rehabilitation. Recent literature focused usually on either the kinematic analysis or on the neurophysiological correlates of robotic rehabilitation. Kinematic data extracted from robotic devices were used to track the patient progress during therapy and predict motor recovery.<sup>15, 16</sup> Changes in cortical activity were monitored by quantitative electroencephalography (EEG).<sup>17, 18</sup> Specifically, resting-state EEG activity, including functional connectivity measures, was correlated with functional recovery, depending on lesion location.<sup>19-21</sup> Cortical reorganization was observed following rehabilitation techniques based on motor learning principles, boosting recovery-related plasticity, both in the sub-acute and

chronic stroke phase.<sup>22</sup> Studies in chronic patients suggested that despite moderate-to-severe impairments, cortical reorganization and gray matter structural changes could be observed after a device-assisted, task-specific upper limb intervention.<sup>23, 24</sup> Few studies also demonstrated the possibility of better capturing patient's motor status by assessing recovery from multiple domains.<sup>25-27</sup> A richer picture of the patient's motor status can be drawn by concomitantly assessing clinical, biomechanical and neurophysiological markers, that features from single domains may not be able to capture.<sup>11</sup> For example, a multimodal approach to post-stroke recovery assessment may correctly identify compensatory behavior, whereas single domain features may not.<sup>26</sup>

Despite the above findings suggesting the possibility to predict the upper limb motor recovery, a comprehensive description of the clinical, kinematic, and brain activity measure following an intensive training at different stages post-stroke is still lacking.

The overall goal of this study is to define the brain activity changes following a 2-week of robotic upper limb treatment protocol in sub-acute and chronic stroke patients, with the aim to further explore the neurophysiological mechanisms underpinning motor recovery. The observed results will help in developing algorithms for predicting recovery and tailor patient-based rehabilitation protocols.

## Materials and methods

### Participants

Ischemic stroke survivors with upper limb paresis were enrolled among inpatients and outpatients from the Neurorehabilitation Unit of Pisa University Hospital, Italy. Participants were recruited in the sub-acute (>10 and <45 days after stroke, abbreviated as SAP) and chronic (>1 year after the event, abbreviated as CHP) phases of the disease. Inclusion criteria were: 1) first-ever unilateral ischemic stroke event; 2) upper limb paresis; 3) age between 18 and 80 years. Exclusion criteria were: 1) upper limb severe spasticity (Modified Ashworth Scale scoring >3) and myoclonus; 2) cognitive impairment (MMSE<24, hemispatial neglect, severe memory/attention impairment or severe aphasia); 3) persistent delirium or disturbed vigilance; 4) new stroke lesion during the rehabilitation period; 5) other neurological complications.

This study was authorized by the local Ethics Committee of Area Vasta Nord Ovest (CEAVNO) for Clinical experimentation, Tuscany (Italy), study number 901/2015. All participants signed their informed consent according to the requirements of the Declaration of Helsinki.

### Study protocol

Participants underwent a robotic rehabilitative treatment of the upper limb. Clinical and neurophysiological assessments were performed within a single session before (T0) and after (T1) the rehabilitative treatment. Kinematic data were acquired during *ad-hoc* pre-treatment and post-treatment evaluation exercises. Clinical and neurophysiological evaluations were repeated one month after the end of the treatment (T2, follow-up). Data were collected by a physician with neurophysiology techniques expertise and a therapist blinded to the patient's allocated condition.

A two-week robotic-aided rehabilitation protocol was applied. The rehabilitation protocol was provided in addition to the usual care, determined on the basis of the patient's needs. The protocol included five treatment sessions per week, using the Mobile roboT for upper limb neuroOrtho Rehabilitation (MOTORE, Humanware Srl, Pisa, Italy), an end-effector robotic device for the assessment and treatment of upper limb motor functions with a virtual interface with visual, acoustic, and strength feedback. Each session lasted approximately one hour. MOTORE allows the execution of task-oriented exercises, performed in active or passive modality. Tasks involved executive functions such as motor control and coordination, problem-solving, and motor planning. The tasks were performed in form of games: examples are a coin collecting game, in which patients were asked to collect virtual coins placed on a semi-circumference or an elliptical trajectory game, in which the subject was asked to follow the trajectory of a virtual car.

The treatment was composed of three phases with increasing difficulty in terms of task complexity, number of repetitions, and amplitude of workspace, to follow the motor improvement of the participants and maximize their engagement and motivation.

Each session was standardized and composed of four parts: passive mode warm-up; pre-treatment active evaluation exercises; treatment active exercises; post-treatment active evaluation exercises. During pre-treatment and post-treatment exercises, kinematics of the end-effector of the robot was recorded.

### Clinical assessments

Participants were characterized with the following clinical scales: Fugl-Meyer Assessment Scale (FMAS) and Wolf Motor Function Test (WMFT). FMAS<sup>28</sup> is an index to global features of impairment in stroke patients, including amplitude of joint movement, pain, sensitivity, motor impairment of the upper and lower extremities, and balance.

Each item is scored on an ordinal three-item scale from 0 to 2 (where 0 = no performance; 2 = complete performance). In our study, we assessed the FMAS for UL only, and considered separately the motor score and the total one (for brevity we will indicate FMAS for UL as "FMAS"). WMFT is used to assess the fine upper limb motor function.<sup>29</sup> Progressing from proximal to distal joint movements, the test consists of 15 timed items and two strength measures. The WMFT-Time measures the time required to complete the task and the WMFT-Score assesses the functional capacity of each task over six levels: 0 indicates that the patient cannot attempt the task, while 5 means that the movement is comparable to the normal one.

### Kinematic assessment

Participants underwent kinematics evaluation before and after each treatment session with the aim to follow the rate of motor learning. The evaluation consisted of a gamified exercise (two repetitions) in which the subject was asked to follow a target moving on an elliptical trajectory by displacing the robot end-effector. The 2-D position of the end-effector of MOTORE was recorded at a sampling frequency of 100 Hz.

To extract kinematics parameters from the data, we applied a third order, 65 samples length Savitzky-Golay filter to smooth the data in the trajectory signal.<sup>30</sup> Smoothed data were visually inspected to discard periods related to arm positioning to the starting location. From the smoothed signal, we extracted six kinematics features: average velocity, average acceleration, percentage of stop time, spectral arc length (SAL), number of peaks in the velocity profile (Npeaks), and total time to complete the task (T-time).<sup>31</sup> The percentage of stop periods was defined as the percentage of time in which the participant moved the robot's end-effector at a speed less than 20% of the maximum speed reached during the assessment. SAL was measured as the arc length of the Fourier-transformed velocity signal in the 0-20 Hz band,<sup>32</sup> while Npeaks was computed using the Matlab function *findpeaks*. The latter two metrics measure the smoothness of the movement. To account for variability in single-session data, we merged the kinematics parameters of the first three rehabilitation sessions ("initial sessions", T0) and the last three sessions ("final sessions", T1) and computed their statistics. We also averaged pre-treatment and post-treatment assessments' data, to obtain patients' performance in each rehabilitation session.

To further investigate the extracted kinematic metrics, we fitted the following function on the mean group evolution of each metric:

$$y = a + b/(1 + e^{ct}) \quad (1)$$

where  $a$ ,  $b$  and  $c$  are parameters to be estimated,  $y$  is the metric considered and  $t$  is the rehabilitation session number. Specifically,  $c$  indicates the rate of motor learning in time, whereas  $a$  and  $b$  are used to adjust for scale and asymptotic value. We bounded  $c$  to be negative for metrics in which better recovery is indicated by a longitudinal decrease in their values. We compared the  $c$  parameter of the fits in the two groups when both showed moderate/high goodness-of-fit ( $R^2 > 0.6$ ).

### Electroencephalographic assessment

The EEG was assessed in resting-state, eyes-closed condition, with participants remaining in a relaxed, seated position for 10 minutes. The EEG was recorded using a 64-channel DC-coupled monopolar amplifier (Micromed SD MRI, System Plus acquisition software), using standard 5% 10/20 system montage. Signals were recorded at a sampling rate of 256 Hz, monitoring the skin-electrode impedance to be lower than 10 k $\Omega$ . To remove electrophysiological and non-electrophysiological artifacts from the raw signals, we used a custom preprocessing pipeline written in MATLAB (MathWorks, Natick, MA, USA) using the EEGLAB toolbox.<sup>33</sup> The pipeline combined two steps of processing:<sup>34</sup> the PREP pipeline,<sup>35</sup> and independent component removal of artifacts.<sup>33</sup> Full details are provided in the Supplementary Digital Material 1 (Supplementary Text File 1). To account for differences in the lesioned hemisphere, we aligned all EEG signals such that right channels referred to the lesioned hemisphere (affected hemisphere, AH), by swapping left and right channels in case of a left-hemisphere lesion.<sup>19, 36</sup>

We then computed an estimate of the power spectral density (PSD) of the signal in each of the recorded channels. We applied Welch's method (averaged periodogram) on 5-s continuous windows of EEG signals, using Hamming windows with no overlap. The spectrum was divided into four frequency bands: Delta (1-4 Hz), Theta (4-8 Hz), Alpha (8-13 Hz), and Beta (13-30 Hz). For each band, the absolute power was first computed by using the trapezoid integration method (MATLAB trapz function), and then normalized to the total power in the frequency range 1-48 Hz (upper limit set to avoid possible residual channel noise activity). Average channel power was computed as the mean power across all electrodes. Moreover, we divided the scalp into six regions of interest (ROIs): frontal right (Fp2, AF4, AF8, F2, F4, F6, F8) frontal left (Fp1, AF3, AF7, F1, F3, F5, F7), central right (FC2, FC4, FC6, FT8,

C2, C4, C6, T4, CP2, CP4, CP6), central left (FC1, FC3, FC5, FT7, C1, C3, C5, T3, CP1, CP3, CP5), occipital right (P2, P4, P6, T6, PO8, PO4, O2) and occipital left (P1, P3, P5, T5, PO7, PO3, O1).<sup>37</sup> ROI power was computed as the average relative power of channels belonging to each ROI.

### Statistical analysis

To evaluate significant changes in clinical tests (dependent variables: FMAS motor and total score and WMFT-score and time), Friedman non-parametric test was used for each group separately (CHP and SAP), to evaluate time (T0, T1, T2) effects. Conover's *post-hoc* comparisons were evaluated. Results from *post-hoc* tests were corrected for multiple comparisons using the Bonferroni-Holm procedure.

To evaluate the evolution of kinematics metrics between initial and final sessions we used a repeated measure analysis of variance model (rmANOVA), with group and time as dependent variables. We also included the interaction term in the model. Whenever the assumption of sphericity was violated (verified by Mauchly Test), the Greenhouse-Geisser correction was applied. *Post-hoc* paired sample *t*-tests (Bonferroni-Holm corrected) were used to check for differences between single time points, within each group. The evolution of spectral parameters was instead evaluated using linear mixed effect models, in which each single-ROI spectral parameter was used as dependent variable, and time (T0, T1 and T2) and group (SAP or CHP) were considered as fixed effects. Subject ID was used as a random effect. By considering each subject as having a different model coefficient, we could obtain a repeated-measure model without removing subjects with missing EEG follow-up assessment. The effects of group, time, and their interaction were evaluated, by adjusting for multiple comparisons using the Bonferroni-Holm method, applied band-wise. Whenever the time or the interaction effect were significant, *post-hoc* paired sample *t*-tests were used to assess time-point differences within groups. We only reported results containing significant *post-hoc* comparisons. Bonferroni-Holm correction was also applied on the *post-hoc* tests. Effect size was evaluated by computing Cohen's  $d$ .

We finally evaluated the potential of spectral metrics as possible markers of the recovery by performing a correlation analysis between the evolution of the relative spectral power in four frequency bands (divided into affected hemisphere, AH, and unaffected hemisphere, UH) and the motor improvement. We used the Spearman correlation coefficient ( $\rho$ ) between the EEG spectral metrics variations and the corresponding motor recovery, as measured by in-



crements of the motor FMAS. We interpreted correlations as follows: low ( $\rho \leq 0.25$ ), moderate ( $0.25 < \rho \leq 0.5$ ), good ( $0.5 < \rho \leq 0.75$ ) and excellent ( $\rho > 0.75$ ).<sup>38</sup> Whenever the correlation resulted good or excellent and its value had the same sign for both SAP and CHP, a common correlation coefficient was computed, shared by both groups. This procedure was applied both to evaluate differences between the end of treatment (T1) and the baseline (T0), and between the follow-up (T2) and the baseline (T0). Ninety-five percent confidence intervals were computed as bias corrected percentile by bootstrapping with  $10^5$  iterations. Significance level was set at 0.05. All analyses were performed using MATLAB R2021a and JASP 0.16.

### Data availability

The data associated with the paper are not publicly available but are available from the corresponding author on reasonable request.

## Results

Thirty-one participants were recruited. Fourteen of them were in the sub-acute phase (SAP) (seven female; mean age:  $64 \pm 14$  years, days from stroke event:  $21.92 \pm 9.59$ ), whereas the other seventeen were chronic stroke partici-

pants (CHP) (five female; mean age:  $59 \pm 13$  years, years from stroke event:  $4.45 \pm 5.72$ ). Demographic and clinical information is reported in Supplementary Digital Material 2 (Supplementary Table I). No differences were present in the age of CHP and SAP (two sample t-test:  $t_{(29)} = 0.935$ ,  $P = 0.35$ ). Kinematic assessments were obtained for 13/14 subacute participants and 12/17 chronic participants: the other participants declined to undergo the assessment tasks. Thirty participants (13/14 SAP and all CHP) performed the EEG evaluation at T0 and T1, whereas 25 participants (10/14 SAP and 14/17 CHP) were collected at T2. The dropout was motivated by patients' refusal to undergo neurophysiological evaluations.

### Clinical assessments

First, we assessed the efficacy of the intensive rehabilitation protocol through clinical scales by using a Friedman Test with paired Conover's *post-hoc* testing for comparing SAP and CHP at T0, T1, and T2. The results are summarized in Supplementary Digital Material 3 (Supplementary Table II). Motor FMAS and total FMAS significantly improved in both SAP and CHP (Figure 1A). A larger effect size improvement is observed in SAP than in CHP (Figure 1B, Supplementary Table II).

WMFT significantly increased in both groups, with a

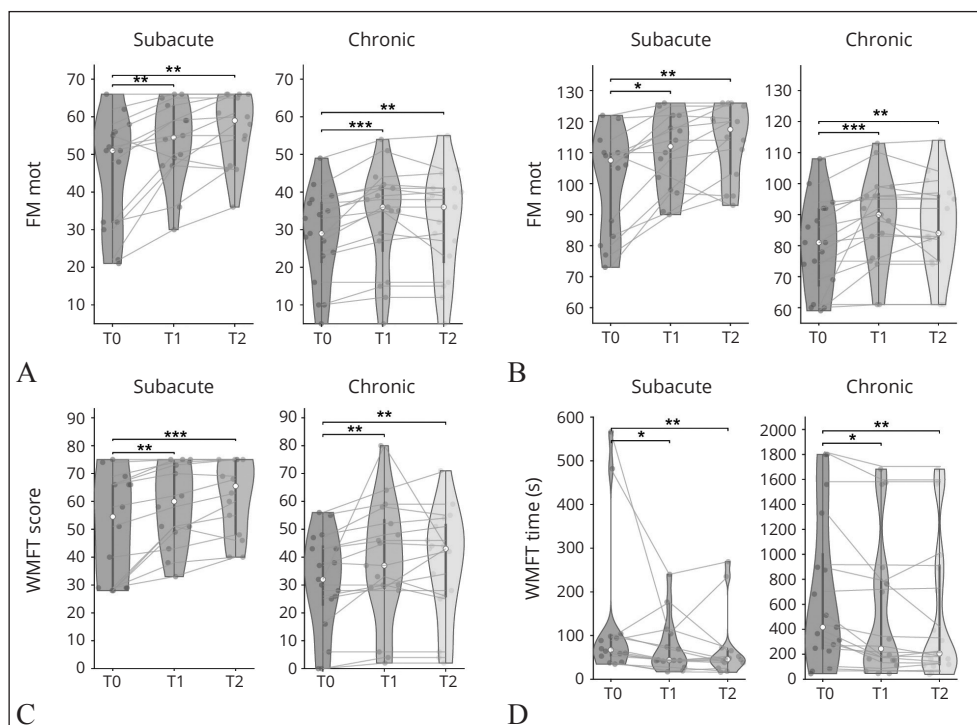


Figure 1.—Clinical scales evaluation in subacute and chronic patients: A) motor subscale of the upper limb FMAS; B) total score of the upper limb FMAS; C) total score of the WMFT; D) total time to complete the WMFT. The significance of the statistical tests is represented as follows: \* $P < 0.05$ , \*\* $P < 0.01$ , \*\*\* $P < 0.001$ . In the violin plots, the inner thick line represents the interquartile range (IQR) of the distribution; the thin line shows the lower/upper adjacent values (first quartile  $-1.5$  IQR and third quartile  $+1.5$  IQR, respectively). Shaded area represents the distribution of the data, as computed by kernel density estimate, and each dot indicates a data point. Grey lines connect data from the same subjects.

significant effect of time, common to both groups. Effect size was again larger in SAP than in CHP (Figure 1C, Supplementary Table II). The recovery was also associated with a significant decrease of the time needed to complete the WMFT (Figure 1D). Overall, both groups showed clinical improvements that are stable at follow-up.

Clinical scales, which reflect the functional ability of the patients, are not able to individuate if improvement can be associated with motor recovery or compensation. Hence, we conducted a thorough kinematic assessment to evaluate how the movements changed during the intervention.

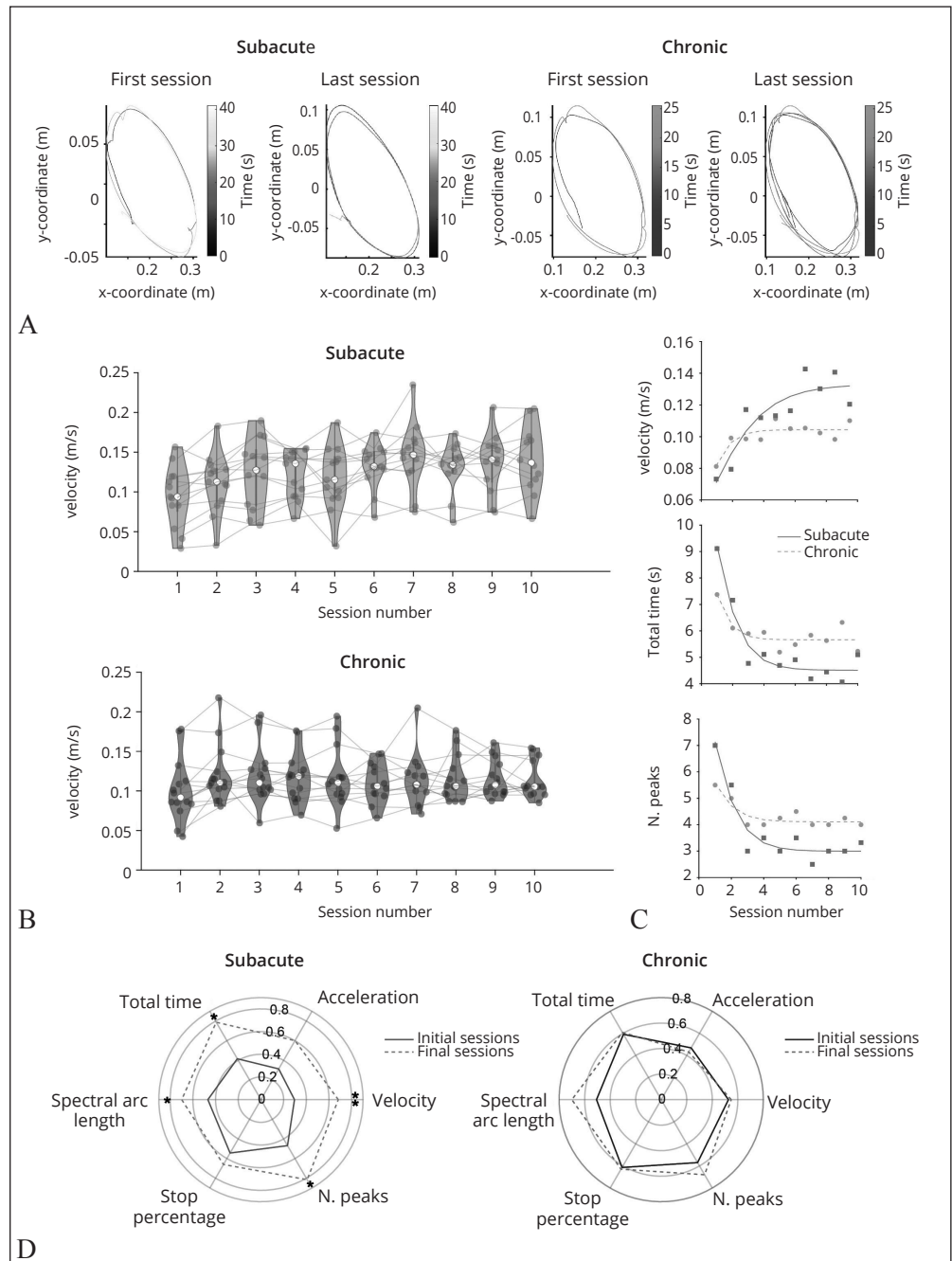


Figure 2.—Kinematics evolution of subacute and stroke patients: A) sample trajectories for one subacute (left) and one chronic (right) participant at the beginning and end of the rehabilitation; B) representative evolution of one of the kinematic metrics (average velocity of movement) over each assessment session after rehabilitation for all patients. Data is represented as violin plots as in the previous figure; C) saturation effects of kinematics metrics; dots indicates mean value of each metric in SA and chronic patients in each session; solid line represents the fitted sigmoidal function; D) spider plot of the evolution between the initial (first three) and final (last three) sessions of rehabilitation for each of the extracted metrics. Each metric was standardized such that each subjects' maximum was set to one before averaging. Metrics having a negative correlation with motor recovery (number of peaks, stop percentage, total time) were reversed. The significance of the corresponding statistical test is represented as follows: \* $P < 0.05$ , \*\* $P < 0.01$ .

### Kinematic assessments

We developed a trajectory task from which we extracted several kinematic parameters that were measured over sessions. Figure 2B shows the evolution of velocity over sessions across patients. This parameter was found to be properly fitted by a plateauing function (SAP  $R^2=0.766$ , CHP  $R^2=0.649$ , Figure 2C). The same result held for Npeaks (SAP  $R^2=0.882$ , CHP  $R^2=0.760$ , Figure 2B) and T-time (SAP  $R^2=0.914$ , CHP  $R^2=0.647$ ) (Figure 2C). CHP reached a plateau earlier than SAP, typically between the 2nd and 4th session as shown by the faster plateauing rate (velocity:  $c=1.205$  for CHP and  $c=0.5050$  for SAP; Npeaks  $c=1.060$ ,  $c=0.958$ ; T-time  $c=1.367$ ,  $c=0.942$ ).

Results on kinematic metrics are reported in Table I. Velocity displayed a significant interaction between factors group and time. A significant effect of time only was observed for Npeaks, SAL and T-time. However, post-hoc testing revealed that differences between initial and final values of these metrics were mostly driven by SAP, which showed a larger effect size and significant differences at the two time-points. Specifically, when compared to T0, at the end of rehabilitation SAP had faster movements, higher SAL, a lower Npeaks, and a lower T-time (Figure 2D). Conversely, none of the kinematic parameters extracted

from the chronic group showed significant improvements. Despite that, effect size was larger for smoothness parameters in this group, namely SAL and Npeaks (Figure 2D). These results suggest that in SAP functional rehabilitation is actually grounded in the recovery of the kinematics of movement, while other mechanisms might contribute for CHP.

### EEG assessment: spectral analysis

We then investigated the neural underpinnings of recovery through EEG analysis at rest. Results are summarized in Figure 3 and Supplementary Digital Material 4 (Supplementary Table III). Both groups showed overall stable average EEG spectra over time (see Figure 3A). However, a significant interaction term between factors group and time was present in the average power of the Beta-band ( $F_{(2,49,13)}=4.052$ ,  $P=0.024$ ). *Post-hoc* testing revealed a significant difference in Beta power only in the SAP group at follow-up compared to baseline (T2-T0: mean difference 0.750,  $t_{(9)}=4.485$ ,  $P=0.005$ , Cohen's  $d=0.340$ ).

We then performed the same analysis separately on each ROI, in the four frequency bands of interest. We did not find any changes in any ROI in Delta (1-4 Hz) and Alpha (8-13 Hz) bands (Figure 3B). Regarding the Beta-band,

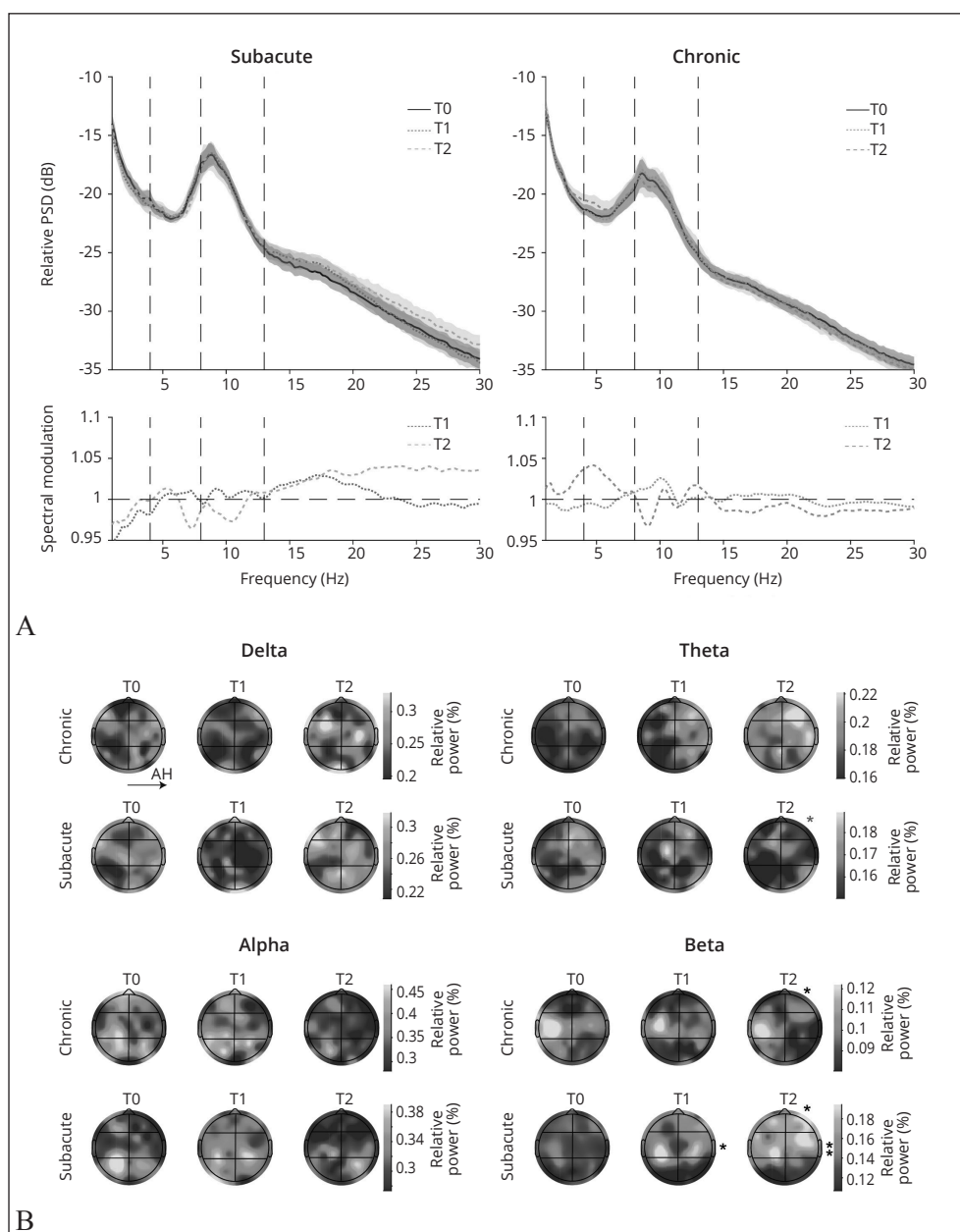
TABLE I.—Results of repeated Measures ANOVA on kinematic metrics.

Dependent variable	Interaction effect	Time effect	SAP T1-T0	CHP T1-T0
Mean velocity	F=7.57 P=0.011*	F=8.50 P=0.007*	$\Delta=0.0279$ $t=3.90$ P=0.002* $d=0.769$	$\Delta=8.1e-4$ T=0.12 P=1.00 $d=0.023$
Mean acceleration	F=3.37 P=0.079	F=3.13 P=0.089	$\Delta=0.067$ $t=2.50$ P=0.115 $d=0.533$	$\Delta=-0.001$ $t=-0.05$ P=1.00 $d=0.007$
SAL	F=0.251 P=0.621	F=6.129 P=0.02*	$\Delta=0.305$ $t=2.35$ P=0.037* $d=0.770$	$\Delta=0.460$ $t=1.69$ P=0.115 $d=0.401$
NPeaks	F=2.559 P=0.122	F=11.437 P=0.002*	$\Delta=-1.832$ $t=-2.85$ P=0.015* $d=0.802$	$\Delta=-0.655$ $t=-1.71$ P=0.111 $d=0.389$
T-Time	F=4.083 P=0.054	F=10.243 P=0.004*	$\Delta=-2.22$ $t=-2.81$ P=0.016* $d=0.784$	$\Delta=-0.502$ $t=0.85$ P=0.866 $d=0.325$
StopPercentage	F=0.619 P=0.439	F=4.254 P=0.050	$\Delta=-4.875$ $t=-1.98$ P=0.332 $d=0.644$	$\Delta=-2.182$ $t=-0.92$ P=1.00 $d=0.153$

SAP: subacute participants; CHP: chronic participants; SAL: spectral arc length; Npeaks: number of peaks in the velocity profile; T-time: total time to complete the task; UH: unaffected hemisphere; AH: affected hemisphere;  $\Delta$ : mean difference;  $d$ : Cohen's  $d$ ;  $P$ : P value;  $F$ : F-test statistic;  $t$ :  $t$ -test statistic.

\*Statistically significant results ( $P<0.05$ ).

Figure 3.—EEG spectral evolution of subacute and chronic stroke patients. A) Top: relative power spectral density averaged across all channels. The solid line shows the mean across all subjects, while shaded area indicates 95% confidence interval of the mean. Bottom: spectral modulation of the mean relative power spectral density of the successive timepoints with reference to the baseline. B) Topographies of power distributions in the two conditions and each time-point in four frequency bands: Delta (1-4 Hz), Theta (4-8 Hz), Alpha (8-13 Hz), Beta (13-30 Hz). Topographies are shown by using the 10/20 standard coordinates on the MNI template. Black lines within the topography represent the edges of the defined ROIs. Power is expressed as the percentage of band power compared to the total power in the range 1-48 Hz. Color bar lower and upper bounds are set to the 5<sup>th</sup> and 95<sup>th</sup> percentile of the power distribution respectively. The significance of the corresponding statistical test (see Methods) is represented as follow side to the significant ROI: \*P<0.05, \*\*P<0.01. A red significance star indicates a significant *post-hoc* test in a quasi-significant linear mixed model interaction coefficient (0.05 < P<0.1).



we observed a significant interaction term between factors group and time in the central area of the AH ROI and a significant time effect in the frontal area of the same hemisphere. From post-hoc testing, SAP showed a significant increase in the ROI of the AH containing motor areas. Additionally, both groups exhibited an increase in the ROI of the AH containing prefrontal areas, which was significant at follow-up. In SAP there was also a significant decrease in the Theta-band power only at T2. Overall, both groups

displayed Beta-band increase during recovery, with the stronger effect on SAP, and only SAP displayed Theta-band decrease in the follow-up.

**EEG assessment: correlation with motor recovery**

Finally, we measured the correlation of the modifications in the power of the frequency bands between T0 and T1 (for both affected hemisphere, AH, and unaffected hemisphere, UH, see Methods) and the increase in motor FMAS



(Figure 4A). In both SAP and CHP Delta-band power anti-correlated with motor FMAS both in the AH and UH (AH:  $\rho=-0.57$ , 95% CI: -0.58, -0.19,  $P=0.004$ ; UH:  $\rho=-0.53$ , 95% CI: -0.74, -0.19,  $P=0.011$ ) (Figure 4B). Alpha-band positively correlated with motor FMAS in UH in SAP

( $\rho=0.56$ ,  $R^2=0.31$ , 95% CI: -0.12, 0.92,  $P=0.24$ ). Any significant correlation was found for Alpha-band in AH for both groups (SAP  $\rho=0.39$ , CHP  $\rho=0.45$ ) and for Theta and Beta-bands in both groups and hemispheres (Supplementary Digital Material 5: Supplementary Table IV, V).

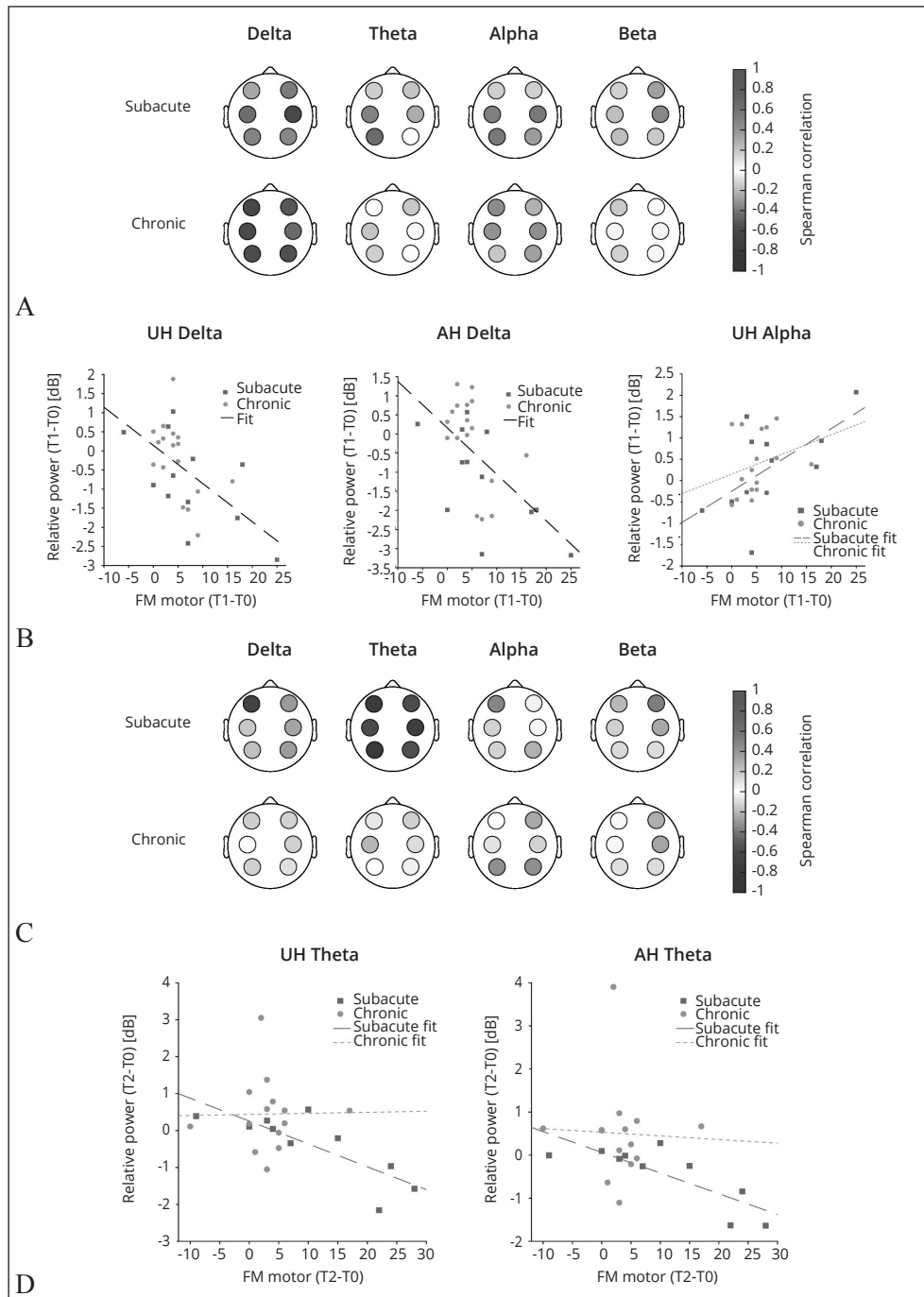


Figure 4.—Correlations between spectral metrics and motor improvement. A) Topographical representation of Spearman correlation between motor improvement (end-of-treatment, T1, vs. baseline, T0) and each ROI changes in relative power in four frequency bands. Each circle represents a ROI. The correlation values are reported in Supplementary Table V. B) Scatter plot representation of significant correlations of spectral measures — divided into affected hemisphere (AH) and unaffected hemisphere (UH) — with motor subscale of the upper limb Fugl-Meyer (T1-T0). Subjects' data are represented as points, colored based on group. Black dashed line indicates the least square fit of the global correlation. If single-group correlation was instead found, a dashed least squares line is shown for each group. C) The same as panel A, but for differences between follow-up (T2) and baseline (T0). D) The same as panel B, but for T2-T0 improvements.

The analysis was repeated for the interval between T2 and T0 and we found an excellent anti-correlation of the FMAS motor improvement with power in the Theta-band, only for SAP, both in AH and UH (AH SAP:  $\rho=-0.76$ , 95% CI: -0.98, -0.094,  $P=0.064$ , UH SAP  $\rho=-0.75$ , 95% CI: -1, -0.21,  $P=0.074$ ) (Figure 4D). The correlation analysis conducted in all other frequency bands was not significant in SAP and CHP (Supplementary Table IV, V).

## Discussion

In this study we aimed to assess the neural mechanisms underlying motor recovery in subacute and chronic stroke patients, affected by upper limb impairment, after an intensive two-week rehabilitation protocol. We measured clinical, kinematics and EEG metrics for each subject before and after the rehabilitation protocol and at one-month follow-up. While clinical scales displayed similar progress in the motor recovery, we found significant differences in the kinematic patterns, with subacute patients reaching better recovery as measured by average velocity and smoothness of the movements. These differences were reflected in the EEG signals, with more pronounced differences appearing in subacute participants throughout the rehabilitation protocol, especially in the Beta-band.

Firstly, the study showed a clinical improvement both in SAP and CHP, showing that an intensive treatment performed with an end-effector device and based on motor and cognitive skill learning principles is able to induce clinical improvement in sub-acute and even in non-recent stroke patients. In the recent years different clinical trials were aimed to demonstrate the existence of a “sensitive period” in which an intensive motor rehabilitation program could provide a heightened motor recovery in stroke patients, with different implications for patients and cost management.<sup>39</sup> Coherently with our evidences, the EXCITE study, a phase III controlled trial, suggests that specific rehabilitative therapies, such as 2 weeks of constraint-induced movement therapy (CIMT), can significantly improve motor function also in the chronic phase after stroke.<sup>40</sup> Conversely, in a recent phase II randomized controlled trial (CPASS study), authors have shown how an “intensive motor training” of the upper extremity (20 hours in addition to standard rehabilitation treatment) was effective only in acute ( $\leq 30$  days after stroke) and sub-acute group (within 60 to 90 days after stroke), while the chronic group (6 months or later after stroke) showed no significant improvement compared with controls. They stated that motor rehabilitation and time post-stroke combine synergical-

ly during a time-limited window to produce enhanced motor recovery.<sup>41</sup> This discrepancy with our study could be explained by non-standardized training since the treatment focused on the use of the more-affected upper extremity in movements mimicking activities of daily living tailored on patients’ needs. In this way every patient performed a treatment agreed with the therapist. Anyway, these conflicting results underline the need to design standardized and repeatable clinical trials able to provide guidelines to the neurorehabilitation community.

Our results also showed that the improvement was greater (in terms of effect size) and was achieved earlier in SAP *versus* CHP. These results confirm the importance of providing a rehabilitative intervention as early as possible, to maximize the recovery of UL functions, in line with previous research.<sup>42, 43</sup> Interestingly, both groups showed retention of improvement after 1 month of training discontinuation, with a stronger effect in SAP. These findings emphasize a “motor learning” mechanism underlying the functional recovery also in chronic patients. However, the greater effect observed in SAP could lead to speculate about a possible different mechanism of cortical plasticity (see below) able to induce a more effective and long-lasting recovery when the subject is treated earlier.

Coherently with clinical analysis, kinematic measures showed an improvement in both groups but a stronger and statistically significant effect in SAP. They showed a reliable improvement in terms of speed and fluidity of movement for the entire duration of treatment. CHP exhibited a rapid plateauing of most kinematic metrics between the 2nd and 4th session. Based on these differences we could assume that motor recovery in our groups could be due to a true recovery in SAP and compensation in CHP.

Our results are also consistent with those showed by Nibras *et al.*<sup>44</sup> They showed that sub-acute stroke patients submitted to upper limb exoskeleton training undergo an overall improvement as measured by clinical scales whereas the kinematic analysis highlighted two clusters of individuals: “recooperer” and “compensator”. The authors declared that recoverers relearned how to generate smooth movements developing synergies similar to those of control participants while compensators improved performance developing compensatory synergies dissimilar to those of controls. We observed the same discrepancy in CHP in which clinical improvement was not followed by a significant improvement in kinematic parameters. Indeed, it has already been described that upper-extremity functional recovery may result from a restored original motor program, but also from new motor patterns arising from an

adaptation of the remaining motor elements or by means compensation through other body segments.<sup>45</sup> These results not only show the importance of an early treatment after stroke, but also highlight how a combination of clinical scales and kinematic assessment is necessary to differentiate between recovery and compensation confirming that a multimodal approach assessing different features of function might provide a more accurate information about patients' abilities and progress.<sup>25</sup>

Our analysis of EEG data highlighted an overall increase in Beta-band activity after treatment in both groups, with a statistically significant result only in SAP. In particular, when we performed a local comparison in the defined ROIs, we found that in SAP the increase in Beta-band activity involves both the primary motor and premotor cortex, whereas in CHP, changes were limited to prefrontal areas. These findings, according with our kinematic results, confirm the hypothesis that SAP were experiencing genuine recovery driven by cortical reorganization in both the primary motor and premotor cortex. On the other hand, the improvement observed in CHP could be potentially driven by compensatory mechanisms, as significant cortical reorganization involved areas not primarily related to motor actions.<sup>43</sup>

Beta-band has been linked to different cognitive functions, such as attention and working memory, and in active motor control.<sup>46, 47</sup> Beta waves seem to be related to the maintenance of the current sensorimotor or cognitive state ("status quo hypothesis").<sup>48</sup> However, the functional relations between Beta, neuronal computation, and behavior remain unclear.<sup>49</sup> Previous studies have explored how motor cortex beta oscillations are affected in patients, at different times after stroke. We have previously shown that during the sub-acute phase of stroke recovery, in absence of a specific rehabilitative intervention, Beta-band power does not correlate with clinical status and intra- and inter-hemispheric Beta-band connectivity is inversely correlated with functional status.<sup>19</sup> Moreover, in chronic stroke patients, we also found a Beta-band increase, over the central region of the affected hemisphere associated with poor motor function. However, in that study, we did not evaluate brain oscillations changes over time or after a specific treatment, so we proposed to interpret Beta-band activity increase as an indirect marker of the brain lesion<sup>50</sup> or due to compensation/maladaptive plasticity. Conversely, Pellegrino *et al.* in 2012 has demonstrated that, following upper limb robotic rehabilitation treatment, an increase in inter-hemispheric functional connectivity in the Beta-band between primary sensorimotor hand areas

is associated with motor recovery.<sup>51</sup> Coherently, Wu *et al.* previously demonstrated that Beta-band power decrease and functional impairment are both driven by neuronal loss following ischemic stroke.<sup>52</sup> Even in the absence of a linear correlation between the extent of Beta-power trend and the clinical improvement, our results are suggestive of an increase of neuronal trafficking induced by treatment. Moreover, Beta-band activity has been previously related to motor learning, both at rest and during tasks. Hence, a modulation of the Beta-band power, specific in the affected hemisphere motor areas, may be related to the undergoing motor learning during the rehabilitation process.<sup>53, 54</sup> Therefore, we could assume that the increase of Beta-band activity in ipsilesional hemisphere represent a direct effect of treatment on cortical rearrangements that are associated with the overall positive outcome in motor recovery.

Regarding low-frequency bands (Delta- and Theta-), previous studies reported association between low-frequency oscillations to volume lesion and injury caused by a stroke event.<sup>55</sup> In our study we found a significant decrease in Theta-band in SAP but only at T2, while no changes were found in Delta-band activity. In the sub-acute phase of stroke the decrease of low-frequency bands was already demonstrated over the ipsilesional central-parietal and supplementary motor area reflecting the improvement of motor networks.<sup>56</sup> The significant difference in the Theta-band observed in our study only at the follow-up is challenging to explain: it may be due to a delayed treatment-induced reorganization or to spontaneous recovery as expected in the SAP group. Anyway, this finding adds knowledge for future studies aimed at using quantitative EEG as biomarker of recovery.

No differences in Delta-band spectral power were observed after our treatment, however when we performed a correlation analysis we found that Delta-band power anti-correlated with motor recovery between T1 and T0, both in AH and UH, in both groups.

The role of Delta-band during stroke recovery was already investigated in a previous study of our group in which we described an asymmetric distribution of Delta activity related to the degree of clinical status in patients with subcortical lesions.<sup>37</sup> This correlation between Delta-band, as well as the Delta/Alpha ratio has already been well described in literature, and different studies showed that Delta-band is significantly negatively associated with motor function.<sup>57, 58</sup> We confirmed the relation between motor recovery (FMAS changes over rehabilitation) and EEG power changes: low-frequency oscillations in Delta band track motor recovery independently from the time

of recovery as SAP and CHP share the same correlational patterns. Another negative correlation in our study was found regarding Theta-band only in SAP between T2 and T0. These data could be related to a delayed effect of rehabilitation per se or to a virtual circle of brain plasticity triggered by the clinical improvement induced by training or by spontaneous mechanisms of brain plasticity expected in SAP.<sup>43</sup> In summary, Delta-band power spectrum reduction is confirmed to be a solid recovery biomarker of motor recovery whereas Theta-band activity is a valid biomarker only in subacute patients and needs more clarification about its significance.

As regards Alpha-band, very interestingly, we found a positive correlation with motor recovery only in UH of SAP group. This seems to confirm the important role of contralesional hemisphere in the recovery mechanisms and how an intensive treatment focused on the affected arm can act in a positive manner on the “health” side of the brain. The role of Alpha-band in the present study spotlights the involvement of the contralesional hemisphere in cortical reorganization mechanisms, and confirms a significant correlation with motor function already described both in early and chronic phase of stroke.<sup>59, 60</sup>

Overall, our research highlights how a multimodal assessment is able to give us a landmark of information necessary to better understand the underpinnings of recovery in stroke patients. This knowledge could pave the way for personalized, precision medicine-based neuro-rehabilitative treatments tailored to the individual characteristics of patients. Future applications of machine learning to clinical, kinematic and neurophysiological data to determine the outcome of rehabilitation therapy for a specific patient profile, but also to identify the optimal predictors of such outcome are desirable to move forward a really impacting effect of rehabilitation on stroke patients’ quality of life.

### Limitations of the study

In our study we proposed two different reorganization patterns after robotic rehabilitative therapy in SAP and CHP. However, in an effort to differentiate true motor recovery from compensatory strategies we have not investigated important measures, such as positive (concentric) joint and total limb power, measures of interlimb (paretic/nonparetic power) and intralimb compensation (shoulder/elbow or shoulder/wrist power), and muscle synergies.

Furthermore, we cannot rule out that the minor kinematic and EEG changes that we observe in the chronic group compared to the subacute one may be due to the limited duration of the rehabilitation protocol (two weeks). Fur-

ther investigations are needed to verify how longer protocols of standardized treatment affect chronic participants. Anyway, our aim was to verify the impact of a short and intensive treatment.

Additionally, it would be desirable to perform the correlation analysis by adding other factors to better depict the underlying processes of recovery, such as age, gender or lesion location.<sup>61</sup> This could add further elements for future applications using machine-learning approaches. Anyway, due to the limited sample size of this study, it was not possible to perform this kind of stratification. Finally, we cannot be conclusive about the specificity of these results due to the end-effector training, as we did not include a control group treated by means of “conventional” therapy.

### Conclusions

In this work we highlighted the neurophysiological and kinematic changes that different stroke survivors’ subpopulations (sub-acute and chronic) undergo after a two-week standardized protocol of robotic rehabilitation. We provide evidence about a different response of cortical reorganization, kinematic modification, and clinical improvement. The combination of these features in a comprehensive evaluation algorithm will help to characterize mechanisms of motor recovery in different phases of stroke patients, and to properly prescribe robot-assisted therapy. An adequate stratification of patients in clinical trials would ensure advances towards precision medicine also in the field of rehabilitation.

### References

1. GBD 2019 Stroke Collaborators. Global, regional, and national burden of stroke and its risk factors, 1990-2019: a systematic analysis for the Global Burden of Disease Study 2019. *Lancet Neurol* 2021;20:795–820.
2. Raghavan P. Upper Limb Motor Impairment After Stroke. *Phys Med Rehabil Clin N Am* 2015;26:599–610.
3. Nichols-Larsen DS, Clark PC, Zeringue A, Greenspan A, Blanton S. Factors influencing stroke survivors’ quality of life during subacute recovery. *Stroke* 2005;36:1480–4.
4. Dobkin BH. Clinical practice. Rehabilitation after stroke. *N Engl J Med* 2005;352:1677–84.
5. Stinear CM, Lang CE, Zeiler S, Byblow WD. Advances and challenges in stroke rehabilitation. *Lancet Neurol* 2020;19:348–60.
6. Frisoli A, Barsotti M, Sotgiu E, Lamola G, Procopio C, Chisari C. A randomized clinical control study on the efficacy of three-dimensional upper limb robotic exoskeleton training in chronic stroke. *J Neuroeng Rehabil* 2022;19:14.
7. Wu J, Cheng H, Zhang J, Yang S, Cai S. Robot-Assisted Therapy for Upper Extremity Motor Impairment After Stroke: A Systematic Review and Meta-Analysis. *Phys Ther* 2021;101:pzab010.



8. Krakauer JW. Motor learning: its relevance to stroke recovery and neurorehabilitation. *Curr Opin Neurol* 2006;19:84–90.
9. Muratori LM, Lamberger EM, Quinn L, Duff SV. Applying principles of motor learning and control to upper extremity rehabilitation. *J Hand Ther* 2013;26:94–102, quiz 103.
10. Boyd LA, Hayward KS, Ward NS, Stinear CM, Rosso C, Fisher RJ, *et al*. Biomarkers of stroke recovery: Consensus-based core recommendations from the Stroke Recovery and Rehabilitation Roundtable. *Int J Stroke* 2017;12:480–93.
11. Maura RM, Rueda Parra S, Stevens RE, Weeks DL, Wolbrecht ET, Perry JC. Literature review of stroke assessment for upper-extremity physical function via EEG, EMG, kinematic, and kinetic measurements and their reliability. *J Neuroeng Rehabil* 2023;20:21.
12. Lohse KR, Lang CE, Boyd LA. Is more better? Using metadata to explore dose-response relationships in stroke rehabilitation. *Stroke* 2014;45:2053–8.
13. Morone G, Palomba A, Martino Cinnera A, Agostini M, Aprile I, Arienti C, *et al*. “CICERONE” Italian Consensus Conference on Robotic in Neurorehabilitation. Systematic review of guidelines to identify recommendations for upper limb robotic rehabilitation after stroke. *Eur J Phys Rehabil Med* 2021;57:238–45.
14. Rozevink SG, Hijmans JM, Horstink KA, van der Sluis CK. Effectiveness of task-specific training using assistive devices and task-specific usual care on upper limb performance after stroke: a systematic review and meta-analysis. *Disabil Rehabil Assist Technol* 2021;1–14.
15. Goffredo M, Pournajaf S, Proietti S, Gison A, Posteraro F, Franceschini M. Retrospective Robot-Measured Upper Limb Kinematic Data From Stroke Patients Are Novel Biomarkers. *Front Neurol* 2021;12:803901.
16. Lee JJ, Shin JH. Predicting Clinically Significant Improvement After Robot-Assisted Upper Limb Rehabilitation in Subacute and Chronic Stroke. *Front Neurol* 2021;12:668923.
17. Finnigan S, van Putten MJ. EEG in ischaemic stroke: quantitative EEG can uniquely inform (sub-)acute prognoses and clinical management. *Clin Neurophysiol* 2013;124:10–9.
18. Rossiter HE, Boudrias MH, Ward NS. Do movement-related beta oscillations change after stroke? *J Neurophysiol* 2014;112:2053–8.
19. Fanciullacci C, Panarese A, Spina V, Lassi M, Mazzoni A, Artoni F, *et al*. Connectivity Measures Differentiate Cortical and Subcortical Sub-Acute Ischemic Stroke Patients. *Front Hum Neurosci* 2021;15:669915.
20. Lamola G, Fanciullacci C, Sgherri G, Bertolucci F, Panarese A, Micera S, *et al*. Neurophysiological Characterization of Subacute Stroke Patients: A Longitudinal Study. *Front Hum Neurosci* 2016;10:574.
21. Saes M, Zandvliet SB, Andringa AS, Daffertshofer A, Twisk JW, Meskers CG, *et al*. Is Resting-State EEG Longitudinally Associated With Recovery of Clinical Neurological Impairments Early Poststroke? A Prospective Cohort Study. *Neurorehabil Neural Repair* 2020;34:389–402.
22. Mooney RA, Cirillo J, Stinear CM, Byblow WD. Neurophysiology of motor skill learning in chronic stroke. *Clin Neurophysiol* 2020;131:791–8.
23. Calabrò RS, Morone G, Naro A, Gandolfi M, Liotti V, D’aurizio C, *et al*. Robot-Assisted Training for Upper Limb in Stroke (ROBOTAS): An Observational, Multicenter Study to Identify Determinants of Efficacy. *J Clin Med* 2021;10:5245.
24. Cho KH, Hong MR, Song WK. Upper limb robotic rehabilitation for chronic stroke survivors: a single-group preliminary study. *J Phys Ther Sci* 2018;30:580–3.
25. Pierella C, Pirondini E, Kinany N, Coscia M, Giang C, Miehlabradt J, *et al*. A multimodal approach to capture post-stroke temporal dynamics of recovery. *J Neural Eng* 2020;17:045002.
26. Belfatto A, Scano A, Chiavenna A, Mastropietro A, Mrakic-Spota S, Pittaccio S, *et al*. A Multiparameter Approach to Evaluate Post-Stroke Patients: An Application on Robotic Rehabilitation. *Appl Sci (Basel)* 2018;8:2248.
27. Comani S, Velluto L, Schinaia L, Cerroni G, Serio A, Buzzelli S, *et al*. Monitoring Neuro-Motor Recovery From Stroke With High-Resolution EEG, Robotics and Virtual Reality: A Proof of Concept. *IEEE Trans Neural Syst Rehabil Eng* 2015;23:1106–16.
28. Fugl-Meyer AR, Jääskö L, Leyman I, Olsson S, Steglind S. The post-stroke hemiplegic patient. 1. a method for evaluation of physical performance. *Scand J Rehabil Med* 1975;7:13–31.
29. Wolf SL, Catlin PA, Ellis M, Archer AL, Morgan B, Piacentino A. Assessing Wolf motor function test as outcome measure for research in patients after stroke. *Stroke* 2001;32:1635–9.
30. Lai S, Panarese A, Spalletti C, Alia C, Ghionzoli A, Caleo M, *et al*. Quantitative kinematic characterization of reaching impairments in mice after a stroke. *Neurorehabil Neural Repair* 2015;29:382–92.
31. Schwarz A, Kanzler CM, Lambercy O, Luft AR, Veerbeek JM. Systematic Review on Kinematic Assessments of Upper Limb Movements After Stroke. *Stroke* 2019;50:718–27.
32. Balasubramanian S, Melendez-Calderon A, Roby-Brami A, Burdet E. On the analysis of movement smoothness. *J Neuroeng Rehabil* 2015;12:112.
33. Delorme A, Makeig S. EEGLAB: an open source toolbox for analysis of single-trial EEG dynamics including independent component analysis. *J Neurosci Methods* 2004;134:9–21.
34. Lassi M, Fabbiani C, Mazzeo S, Burali R, Vergani AA, Giacomucci G, *et al*. Degradation of EEG microstates patterns in subjective cognitive decline and mild cognitive impairment: early biomarkers along the Alzheimer’s Disease continuum? *Neuroimage Clin* 2023;38:103407.
35. Bigdely-Shamlo N, Mullen T, Kothe C, Su KM, Robbins KA. The PREP pipeline: standardized preprocessing for large-scale EEG analysis. *Front Neuroinform* 2015;9:16.
36. Pichiorri F, Petti M, Caschera S, Astolfi L, Cincotti F, Mattia D. An EEG index of sensorimotor interhemispheric coupling after unilateral stroke: clinical and neurophysiological study. *Eur J Neurosci* 2018;47:158–63.
37. Fanciullacci C, Bertolucci F, Lamola G, Panarese A, Artoni F, Micera S, *et al*. Delta Power Is Higher and More Symmetrical in Ischemic Stroke Patients with Cortical Involvement. *Front Hum Neurosci* 2017;11:385.
38. Portney LG. Foundations of Clinical Research: Applications to Evidence-Based Practice. Fourth edition. Philadelphia: F.A. Davis Co; 2020.
39. Dromerick AW, Edwardson MA, Edwards DF, Giannetti ML, Barth J, Brady KP, *et al*. Critical periods after stroke study: translating animal stroke recovery experiments into a clinical trial. *Front Hum Neurosci* 2015;9:231.
40. Wolf SL, Thompson PA, Winstein CJ, Miller JP, Blanton SR, Nichols-Larsen DS, *et al*. The EXCITE stroke trial: comparing early and delayed constraint-induced movement therapy. *Stroke* 2010;41:2309–15.
41. Dromerick AW, Geed S, Barth J, Brady K, Giannetti ML, Mitchell A, *et al*. Critical Period After Stroke Study (CPASS): A phase II clinical trial testing an optimal time for motor recovery after stroke in humans. *Proc Natl Acad Sci USA* 2021;118:e2026676118.
42. Langhorne P, Bernhardt J, Kwakkel G. Stroke rehabilitation. *Lancet* 2011;377:1693–702.
43. Murphy TH, Corbett D. Plasticity during stroke recovery: from synapse to behaviour. *Nat Rev Neurosci* 2009;10:861–72.
44. Nibras N, Liu C, Mottet D, Wang C, Reinkensmeyer D, Remyneris O, *et al*. Dissociating Sensorimotor Recovery and Compensation During Exoskeleton Training Following Stroke. *Front Hum Neurosci* 2021;15:645021.
45. Levin MF, Kleim JA, Wolf SL. What do motor “recovery” and “compensation” mean in patients following stroke? *Neurorehabil Neural Repair* 2009;23:313–9.
46. Lundqvist M, Rose J, Herman P, Brincat SL, Buschman TJ, Miller EK. Gamma and Beta Bursts Underlie Working Memory. *Neuron* 2016;90:152–64.
47. Tan H, Wade C, Brown P. Post-Movement Beta Activity in Sensorimotor Cortex Indexes Confidence in the Estimations from Internal Models. *J Neurosci* 2016;36:1516–28.

48. Engel AK, Fries P. Beta-band oscillations—signalling the status quo? *Curr Opin Neurobiol* 2010;20:156–65.
49. Peles O, Werner-Reiss U, Bergman H, Israel Z, Vaadia E. Phase-Specific Microstimulation Differentially Modulates Beta Oscillations and Affects Behavior. *Cell Rep* 2020;30:2555–2566.e3.
50. Thibaut A, Simis M, Battistella LR, Fanciullacci C, Bertolucci F, Huerta-Gutierrez R, *et al.* Using Brain Oscillations and Corticospinal Excitability to Understand and Predict Post-Stroke Motor Function. *Front Neurol* 2017;8:187.
51. Pellegrino G, Tomasevic L, Tombini M, Assenza G, Bravi M, Sterzi S, *et al.* Inter-hemispheric coupling changes associate with motor improvements after robotic stroke rehabilitation. *Restor Neurol Neurosci* 2012;30:497–510.
52. Wu J, Srinivasan R, Burke Quinlan E, Solodkin A, Small SL, Cramer SC. Utility of EEG measures of brain function in patients with acute stroke. *J Neurophysiol* 2016;115:2399–405.
53. Sugata H, Yagi K, Yazawa S, Nagase Y, Tsuruta K, Ikeda T, *et al.* Role of beta-band resting-state functional connectivity as a predictor of motor learning ability. *Neuroimage* 2020;210:116562.
54. Aliakbaryhosseinabadi S, Lontis R, Farina D, Mrachacz-Kersting N. Effect of motor learning with different complexities on EEG spectral distribution and performance improvement. *Biomed Signal Process Control* 2021;66:102447.
55. Cassidy JM, Wodeyar A, Wu J, Kaur K, Masuda AK, Srinivasan R, *et al.* Low-Frequency Oscillations Are a Biomarker of Injury and Recovery After Stroke. *Stroke* 2020;51:1442–50.
56. Gyulai A, Körmendi J, Juhasz Z, Nagy Z. Inter trial coherence of low-frequency oscillations in the course of stroke recovery. *Clin Neurophysiol* 2021;132:2447–55.
57. Leon-Carrion J, Martin-Rodriguez JF, Damas-Lopez J, Barroso y Martin JM, Dominguez-Morales MR. Delta-alpha ratio correlates with level of recovery after neurorehabilitation in patients with acquired brain injury. *Clin Neurophysiol* 2009;120:1039–45.
58. Assenza G, Zappasodi F, Pasqualetti P, Vernieri F, Tecchio F. A contralesional EEG power increase mediated by interhemispheric disconnection provides negative prognosis in acute stroke. *Restor Neurol Neurosci* 2013;31:177–88.
59. Cassidy JM, Wodeyar A, Srinivasan R, Cramer SC. Coherent neural oscillations inform early stroke motor recovery. *Hum Brain Mapp* 2021;42:5636–47.
60. Shim M, Choi GY, Paik NJ, Lim C, Hwang HJ, Kim WS. Altered Functional Networks of Alpha and Low-Beta Bands During Upper Limb Movement and Association with Motor Impairment in Chronic Stroke. *Brain Connect* 2023;13:487–97.
61. Alawieh A, Zhao J, Feng W. Factors affecting post-stroke motor recovery: implications on neurotherapy after brain injury. *Behav Brain Res* 2018;340:94–101.

#### Conflicts of interest

The authors certify that there is no conflict of interest with any financial organization regarding the material discussed in the manuscript.

#### Funding

This work was supported by the PERSONA Project, which is funded by Regione Toscana – Bando Salute 2018. This work was partly funded by the Bertarelli Foundation ([www.fondation-bertarelli.org](http://www.fondation-bertarelli.org)). The project was also funded under the National Recovery and Resilience Plan (NRRP), Mission 4 Component 2 Investment 1.3 - Call for tender No. 341 of 15/03/2022 of Italian Ministry of University and Research funded by the European Union – NextGenerationEU, award Number: Project code PE0000006, Concession Decree No. 1553 of 11/10/2022 adopted by the Italian Ministry of University and Research, CUP D93C22000930002, “A multiscale integrated approach to the study of the nervous system in health and disease” (MNESYS). The funders had no role in study design, data collection and analysis, decision to publish, or preparation of the manuscript.

#### Authors' contributions

Michael Lassi and Stefania Dalise contributed equally to this work. Carmelo Chisari, Stefania Dalise, Alberto Mazzoni and Silvestro Micera participated in the study conception and design. Stefania Dalise, Vincenzo Spina and Valentina Azzollini performed the recruitment of study participants and data collection. Michael Lassi, Andrea Bandini and Matteo Vissani performed the data analysis. Michael Lassi, Andrea Bandini and Stefania Dalise drafted the manuscript. All authors contributed to the critical discussion of the obtained results, read and approved the final version of the manuscript.

#### History

Article first published online: November 21, 2023. - Manuscript accepted: October 20, 2023. - Manuscript revised: September 6, 2023. - Manuscript received: February 14, 2023.

**Supplementary Methods: EEG pre-processing**

The PREP pipeline performed several preprocessing steps automatically and allowed us to obtain robust averaged-referenced signals. These steps included: () PREP high-pass filtering of all channels, using a Hamming windowed FIR filter (EEGLAB's `pop_eegfiltnew` function) with a 1 Hz cut-off frequency; 2) line noise removal (50 Hz and its harmonics) via the CleanLine EEGLAB plugin; 3) noisy channel removal (*i.e.*, channels with abnormal and/or uncorrelated activity compared to others) with the PREP noisy channel subroutine, which performs the bad channel selection by combining an ensemble of methods that include the deviation criterion, the correlation criterion, the noisiness criterion, and the predictability criterion; 4) the remaining channel activity was used to estimate a robust average reference, based on robust statistics such as the median and interquartile range; 5) the removed channels were interpolated using spherical interpolation.

The re-referenced and filtered signals were processed with the second preprocessing step. Independent components were extracted by using the Infomax ICA algorithm,<sup>1</sup> as implemented in the “*binica*” EEGLAB routine. A semi-automated procedure was then used to distinguish between brain-related components and artifactual ones. We used ICLabel to automatically classify the independent components as brain or artifactual components (*i.e.*, line noise, muscle, eye, channel noise, heart, other) based on a neural network trained on crowd-sourced data.<sup>2</sup> ICLabel returns the probability of each component belonging to one of the above-mentioned classes. Afterward, we used DIPFIT to perform a single dipole fitting of the independent component map onto a template brain (MNI-152 atlas). Given that brain components should be dipolar,<sup>3</sup> a high residual variance of the fitted dipole should indicate a low probability of the component being brain-related. Hence, components labeled by ICLabel as “brain” with a confidence higher than a threshold (we used 75%) and having fitted dipole residual variance lower than another threshold (we used 20%) were retained in the final signals. Noise components with high confidence and high dipole residual variance were instead automatically removed from the ICs list. All the remaining components were visually inspected and flagged either as brain or non-brain depending on their power spectra profiles and time courses. Channel-level signals were finally reconstructed from the reduced IC space, only including brain-related sources.

Finally, we performed a visual inspection of the cleaned signals, to remove possible remaining artifacts (*e.g.*, temporally localized muscle activity not removed by the ICA procedure). If portions of the signal were removed at this last preprocessing step, another round of ICA pruning was performed, to verify whether the found components were of neural origin and possibly remove other noisy components.

1. Bell AJ, Sejnowski TJ. An information-maximization approach to blind separation and blind deconvolution. *Neural Comput.* 1995 Nov;7(6):1129–59.
2. Pion-Tonachini L, Kreutz-Delgado K, Makeig S. ICLabel: An automated electroencephalographic independent component classifier, dataset, and website. *NeuroImage.* 2019 Sep;198:181–97.
3. Delorme A, Palmer J, Onton J, Oostenveld R, Makeig S. Independent EEG Sources Are Dipolar. *PLOS ONE.* 2012 Feb 15;7(2):e30135.

SUPPLEMENTARY DIGITAL MATERIAL 2

Supplementary Table I.—Stroke patients' baseline characteristics.

Patient	Age	Gender	Lesion side/Location	Group	Time since stroke	FMA-UL MF	FMA-UL TOT	WMFT Score	WMFT Time (s)
1	65	M	L/Centrum semioval	Subacute	32 days	21	77	29	482
2	22	M	L/Internal capsule	Subacute	21 days	62	122	66	39
3	82	F	R/Internal capsule	Subacute	27 days	48	106	58	104
4	59	M	R/Fronto-parieto-occipital	Subacute	19 days	51	109	66	98.2
5	61	F	R/Fronto-temporo-parietal	Subacute	14 days	66	121	74	52.9
6	61	F	R/Nucleus caudatus	Subacute	20 days	58	114	69	64.2
7	66	M	L/Temporo-parietal	Subacute	19 days	56	105	75	69.9
8	60	F	L/Centrum semiovale	Subacute	10 days	22	73	28	566.4
9	67	M	R/Internal capsule	Subacute	23 days	52	109	66	58.6
10	59	M	L/Insula and frontal	Subacute	45 days	30	80	29	37.5
11	70	F	R/pons	Subacute	11 days	51	110	51	34.5
12	72	M	L/NA	Subacute	28 days	55	110	40	59.4
13	70	F	R/Perirolandic	Subacute	22 days	32	83	29	88.5
14	79	F	L/Perirolandic	Subacute	14 days	32	88	28	94.5
15	84	F	L/ND	Chronic	24 years	35	92	48	417
16	83	F	R/Corona Radiata	Chronic	1 year	42	100	47	314
17	59	M	R/ND	Chronic	2 years	49	108	56	64
18	85	F	L/ND	Chronic	6 years	38	92	37	512
19	54	M	L/bulbus-pons	Chronic	2 years	34	88	43	248
20	59	M	R/Fronto-temporo-parietal	Chronic	6 years	39	81	43	227
21	78	M	L/ND	Chronic	2 years	10	60	0	1800
22	63	M	R/Corona radiata	Chronic	5 years	16	75	28	896.6
23	65	M	L/Insula	Chronic	1 year	10	59	0	1800
24	22	M	R/Prerolandic	Chronic	2 years	27	81	55	365
25	82	F	L/Internal capsule	Chronic	1.5 years	29	74	16	1330.5
26	52	M	L/Corona radiata	Chronic	1 year	37	94	32	681.7
27	73	M	L/Internal capsule	Chronic	3 years	5	61	6	1560.2
28	80	M	R/Internal capsule	Chronic	2 years	24	78	25	875.1
29	77	M	L/Temporo-parietal	Chronic	9 years	23	69	30	83.9
30	71	M	R/Internal capsule	Chronic	1 year	28	60	38	277.4
31	70	M	R/Internal capsule	Chronic	2.5 years	33	86	26	44.9

F: female; M: male; L: left; R: right; FMA-UL MF: Fugl-Meyer Assessment Upper Limb Motor Function; FMA-UL TOT: Fugl-Meyer Assessment Upper Limb Total Score; WMFT: Wolf Motor Function Test.



SUPPLEMENTARY DIGITAL MATERIAL 3

Supplementary Table II.—Results of repeated Measures ANOVA on clinical scales. Bold cells are significant results (P<0.05).

Dependent variable	SAP time effect	SAP	SAP	SAP	CHP time effect	CHP	CHP	CHP
		T1 – T0	T2 – T0	T2 – T1		T1 – T0	T2 – T0	T2 – T1
FMAS motor	$\chi=16.29$	$\Delta=7.86$	$\Delta=11.14$	$\Delta=3.29$	$\chi=21.71$	$\Delta=4.77$	$\Delta=3.59$	$\Delta=-1.18$
	P<0.001	t=2.74	t=3.96	t=1.22	P<0.001	t=4.32	t=3.75	t=0.58
		P=0.022	P=0.002	P=0.234		P<0.001	P=0.001	P=0.568
FMAS total	$\chi=15.22$	$\Delta=9.50$	$\Delta=13.21$	$\Delta=3.714$	$\chi=21.71$	$\Delta=7.88$	$\Delta=6.71$	$\Delta=-1.18$
	P<0.001	t=2.78	t=3.78	t=0.99	P<0.001	t=4.32	t=3.75	t=0.58
		P=0.020	P=0.003	P=0.329		P<0.001	P=0.001	P=0.568
WMFT score	$\chi=22.24$	$\Delta=8.50$	$\Delta=11.14$	$\Delta=2.643$	$\chi=17.13$	$\Delta=7.12$	$\Delta=6.12$	$\Delta=-1.00$
	P< 0.001	t=3.22	t=4.62	t=1.41	P<0.001	t=3.46	t=3.75	t=0.29
		P=0.007	P<0.001	P=0.171		P=0.003	P=0.002	P=0.775
WMFT time	$\chi=16.00$	$\Delta=-56.73$	$\Delta=-59.98$	$\Delta=-3.26$	$\chi=13.58$	$\Delta=-121.11$	$\Delta=-132.11$	$\Delta=-11.01$
	P<0.001	t=3.02	t=3.78	t=0.76	P=0.001	t=2.79	t=-3.49	t=0.70
		P=0.011	P=0.002	P=0.456		P=0.018	P=0.004	P=0.491
		d=0.445	d=0.457	d=0.045		d=0.206	d=0.223	d=0.019

FMAS: Fugl-Meyer Assessment Upper Limb; WMFT: WMFT: Wolf Motor Function Test; SAP: subacute participants; CHP: chronic participants; UH: unaffected hemisphere; AH: affected hemisphere;  $\Delta$ : mean difference; d: Cohen's d; P: P value;  $\chi$ : chi-squared test statistic; t: Conover's test statistic.

\*The statistics are computed on both groups together and hence reported only once.

SUPPLEMENTARY DIGITAL MATERIAL 4

Supplementary Table III.—Results of linear mixed effects model on EEG metrics (only significant *post-hoc* results are reported, see Figure 3B). F-statistic degrees of freedom are (2.49, 13).

Dependent variable	Interaction effect	Time effect	SAP T1 – T0	SAP T2 – T0	SAP T2 – T1	CHP T1 – T0	CHP T2 – T0	CHP T2 – T1
Central AH Beta	F=4.90 P=0.048	F=3.05 p=0.226	$\Delta$ =-0.527	$\Delta$ =-0.96	$\Delta$ =-0.43	$\Delta$ =-0.16	$\Delta$ =-0.34	$\Delta$ =-0.18
			t=2.49	t=4.46	t=2.60	t=-0.59	t=-0.53	t=0.14
			P=0.03	P=0.005	P=0.057	P=1	P=1	P=0.894
Frontal AH Beta	F=2.37 P=0.416	F=4.961 P=0.044	d=0.219	d=0.443	d=0.198	d=0.060	d=0.142	d=0.072
			$\Delta$ =0.123	$\Delta$ =0.417	$\Delta$ =0.176	*	*	*
			t=1.15	t=2.59	t=1.66			
Frontal AH Theta	F=4.424 P=0.068	F=0.401 P=1	P=0.259	P=0.049	P=0.220			
			d=0.092	d=0.170	d=0.071			
			$\Delta$ =-0.122	$\Delta$ =-0.490	$\Delta$ =-0.36	$\Delta$ =0.09	$\Delta$ =0.489	$\Delta$ =0.397
			t=-0.54	t=-3.01	t=-2.21	t=0.39	t=1.60	t=0.88
			P=0.599	P=0.044	P=0.108	P=0.702	P=0.399	P=0.794
			d=0.085	d=0.307	d=0.282	d=0.034	d=0.177	d=0.140

SAP: subacute participants; CHP: chronic participants; UH: unaffected hemisphere; AH: affected hemisphere;  $\Delta$ : mean difference; d: Cohen's d; P: P value; F: F-test statistic; t: t-test statistic.

\*The statistics are computed on both groups together and hence reported only once.



Supplementary Table V.—Spearman correlation between EEG bands and clinical improvements in the defined ROIs.

T1 - T0					
Subacute	Chronic		Chronic	Chronic	
	UH	AH		UH	AH
Frontal Delta	-0.253079089	-0.39016	Frontal Delta	-0.61931	-0.52042
Frontal Theta	-0.140599494	-0.1652	Frontal Theta	-0.00371	-0.15946
Frontal Alpha	0.168719393	0.168719	Frontal Alpha	0.457372	0.275659
Frontal Beta	0.17223438	0.355014	Frontal Beta	-0.14957	-0.01236
Central Delta	-0.435858431	-0.61161	Central Delta	-0.59211	-0.44872
Central Theta	-0.372588658	-0.24253	Central Theta	-0.16935	0.017306
Central Alpha	0.51670314	0.558883	Central Alpha	0.426468	0.432649
Central Beta	0.228474177	0.481553	Central Beta	0.034612	0.03214
Posterior Delta	-0.362043696	-0.35853	Posterior Delta	-0.57604	-0.55255
Posterior Theta	-0.446403393	0	Posterior Theta	-0.13598	-0.00865
Posterior Alpha	0.558882988	0.376104	Posterior Alpha	0.199019	0.346119
Posterior Beta	0.231989165	-0.15114	Posterior Beta	0.15699	-0.02349
T2 - T0					
Subacute	Chronic		Chronic	Chronic	
	UH	AH		UH	AH
Frontal Delta	-0.672727273	-0.29697	Frontal Delta	-0.13732	0.150614
Frontal Theta	-0.806060606	-0.57576	Frontal Theta	-0.06645	-0.12625
Frontal Alpha	0.490909091	0.042424	Frontal Alpha	-0.00221	-0.25028
Frontal Beta	0.248484848	0.527273	Frontal Beta	-0.01772	-0.23478
Central Delta	-0.163636364	-0.26061	Central Delta	-0.00443	0.161688
Central Theta	-0.575757576	-0.73333	Central Theta	-0.2082	-0.09081
Central Alpha	0.151515152	0.030303	Central Alpha	-0.07752	-0.12182
Central Beta	0.163636364	0.321212	Central Beta	0.026579	-0.26136
Posterior Delta	-0.187878788	-0.28485	Posterior Delta	0.157258	0.101886
Posterior Theta	-0.83030303	-0.55152	Posterior Theta	0	-0.04208
Posterior Alpha	0.151515152	0.284848	Posterior Alpha	-0.33667	-0.33224
Posterior Beta	-0.103030303	0.115152	Posterior Beta	0.099671	0.110745